

# RSC Advances



This is an *Accepted Manuscript*, which has been through the Royal Society of Chemistry peer review process and has been accepted for publication.

*Accepted Manuscripts* are published online shortly after acceptance, before technical editing, formatting and proof reading. Using this free service, authors can make their results available to the community, in citable form, before we publish the edited article. This *Accepted Manuscript* will be replaced by the edited, formatted and paginated article as soon as this is available.

You can find more information about *Accepted Manuscripts* in the [Information for Authors](#).

Please note that technical editing may introduce minor changes to the text and/or graphics, which may alter content. The journal's standard [Terms & Conditions](#) and the [Ethical guidelines](#) still apply. In no event shall the Royal Society of Chemistry be held responsible for any errors or omissions in this *Accepted Manuscript* or any consequences arising from the use of any information it contains.

Cite this: DOI: 10.1039/c0xx00000x

www.rsc.org/xxxxxx

## Highly thermal conductivity graphite nanoplatelets/UHMWPE nanocomposites

Junwei Gu\*, Nan Li, Lidong Tian, Zhaoyuan Lv, Qiuyu Zhang\*

Key Laboratory of Space Applied Physics and Chemistry, Ministry of Education, Department of Applied Chemistry, School of Science, Northwestern Polytechnical University, Xi'an, Shaan Xi 710072, P. R. China. Corresponding author to J.W. Gu & Q.Y. Zhang, E-mail address: nwpugjw@163.com & qyzhang1803@gmail.com; Tel: +86-29-88431621.

Highly thermal conductivity graphite nanoplatelets/ultra high molecular weight polyethylene (GNPs/UHMWPE) nanocomposites are fabricated via mechanical ball milling followed by hot-pressing method. GNPs are located on the interface of UHMWPE matrix. The thermal conductive coefficient of the GNPs/UHMWPE nanocomposite is greatly improved to 4.624 W/ mK with 21.4 vol% GNPs, 9 times higher than that of original UHMWPE matrix. The significantly high improvement of the thermal conductivity is ascribed to the formation of multidimensional thermal conductive networks of GNPs-GNPs, and GNPs have strong ability to form continuous thermal conductive networks. The cooling-pressing along with the machine is more beneficial for the improvement of thermal conductivity, by increasing the crystallinity of UHMWPE matrix. Furthermore, the thermal stabilities of the GNPs/UHMWPE nanocomposites are increased with the increasing addition of GNPs.

### Introduction

The integration and miniaturization of microelectronic devices put higher requirement for advanced microelectronic packaging materials<sup>1-6</sup>. Against this background, highly thermal conductivity polymeric composites possess significant potential in the advanced microelectronic packaging, which requires good heat dissipation, low thermal expansion and light weight<sup>7, 8</sup>. However, the thermal conductive coefficient of polymeric matrix is much lower than that for metals or ceramic materials. Recent studies have revealed that by incorporation thermal conductive fillers, such as graphene<sup>9-12</sup>, carbon nanotube<sup>13-16</sup>, boron nitride nanotube<sup>17</sup>, silicon nitride<sup>18-20</sup>, silicon carbide<sup>21-22</sup> and graphite<sup>1, 23-25</sup>, etc., into polymeric matrix can effectively increase the thermal conductivities of the composites. In our previous work<sup>26-31</sup>, several thermal conductive polymeric composites have been fabricated successfully by adding single or hybrid thermal conductive fillers. However, the improvement of thermal conductivities of the composites is often less than expected from previous theory design. Furthermore, to fabricate polymeric composites with highly thermal conductivity higher than 4 W/mK, the addition of thermal conductive fillers is typically beyond 30 vol%, which creates a significant challenge of processing behavior, mechanical properties and density<sup>32</sup>. According to the heat-transfer mechanism of lattice vibration, collision probability of phonon is smaller and the average free path of phonon is larger spreading in the crystalline region<sup>33</sup>. Therefore, the crystallinity of polymers strongly affects the

thermal conductivity, from 0.2 W/mK for amorphous polymers to 0.5 W/mK for highly crystalline polymers<sup>34</sup>. For this reason, the improvement of crystallinity is emerging as one of the most effective ways to increase the intrinsic thermal conductivity of polymeric matrix. The more recognized thermal conductive mechanism is that the thermal transport through not only thermal conductive networks of fillers, but also the polymeric matrix. And the thermal conductive percolation behavior plays a major role in the great enhancement of the thermal conductivities<sup>35, 36</sup>. To our best knowledge, a low percolation threshold can be achieved for the polymeric composites with segregated structures, which thermal conductive fillers are located on the interface of polymeric matrix instead of being randomly distributed in the polymeric matrix<sup>37, 38</sup>. Ultra-high molecular weight polyethylene (UHMWPE) is an engineering thermoplastic, replacing the existing conventional polyethylene, due to its outstanding wear resistance, excellent chemical stability & low friction, good self-lubricating properties & bio-compatibility, as well as surprising impact toughness, etc., which has great applications in the fields of transportation, agriculture, medicine, food, chemical, textile, paper making, aerospace industry and defense military equipments<sup>39-41</sup>. Additionally, owing to super diameter/thickness ratio, outstanding physical properties and cost efficiency, graphite nanoplatelets (GNPs) are considered to be effective fillers for fabricating polymeric composites with a relative higher thermal conductivity as compared to graphene, carbon nanotube and boron nitride nanotube<sup>1, 26, 42-45</sup>. Work by Kalaitzidou and coworkers<sup>46</sup> has also

shown that GNPs can obviously enhance the thermal conductivity of the polypropylene (PP). The maximum thermal conductivity value measured for 25 vol% GNPs/PP composites was 6 times higher than that of original PP.

In our present work, the method of mechanical ball milling followed by hot-pressing is introduced to fabricate the highly thermal conductive GNPs/UHMWPE nanocomposites with segregated structures. And the cooling-pressing along with the machine after hot-pressing is also adopted to further increase the thermal conductivities of the GNPs/UHMWPE nanocomposites by further improving the crystallinity of UHMWPE matrix. And the thermal conductivities and thermal stabilities of the GNPs/UHMWPE nanocomposites are also investigated.

## Materials and Methods

### Materials

Graphite nanoplatelets (GNPs), KNG-180, with diameter of 40  $\mu\text{m}$ , super diameter/thickness ratio of 250, are received from Xiamen Knano Graphene Technology Co. Ltd. (Fujian, China); Ultra high molecular weight polyethylene (UHMWPE), powdery,  $0.97 \text{ g/cm}^3$ , mean particle size of 60  $\mu\text{m}$ , is supplied by Nanjing Deyuan Science and Technology Co. Ltd. (Jiangsu, China); Tetrahydrofuran (THF) and absolute ethanol are all purchased from Tianjin Ganglong Chemical Group Co., Ltd. (Tianjin, China).

### Preparation of the GNPs/UHMWPE nanocomposites

Pristine GNPs are firstly immersed in THF and absolute ethanol for 12 hrs at room temperature for each step to effectively remove other impurities on the surface of GNPs, followed by storage at  $60^\circ\text{C}$  vacuum oven for 24 hrs. UHMWPE is firstly dried in vacuum oven at  $60^\circ\text{C}$  for 6 hrs. And the GNPs/UHMWPE nanocomposites are fabricated according to the following procedures: (i) Mixing GNPs and UHMWPE matrix using ball milling machine for 24 hrs at room temperature, to embed the GNPs onto the interface of UHMWPE matrix; (ii) Hot-pressing ( $195^\circ\text{C}/10\text{MPa}$ ) to fabricate the GNPs/UHMWPE with segregated structures. Herein, GNPs are located on the interface of UHMWPE. (Schematic diagram in Fig.1).

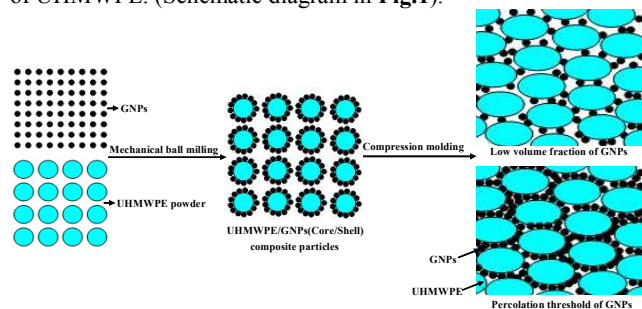


Fig.1 Schematic diagram of thermal conductive mechanism of the GNPs/UHMWPE nanocomposites

And two methods of “direct cooling-pressing away from the machine” and “cooling-pressing along with the machine” are performed after hot-pressing ( $195^\circ\text{C}/10\text{MPa}$ ). Herein, the former is firstly hot-pressed under  $195^\circ\text{C}$  at  $10\text{MPa}$  for 15 min, and then the metal mold is directly removed from the press to room temperature environment quickly under specific pressure. And the latter is firstly hot-pressed under  $195^\circ\text{C}$  at  $10\text{MPa}$  for 15 min,

and then the press is powered off, but the metal mold is still placed on the press under specific pressure to room temperature.

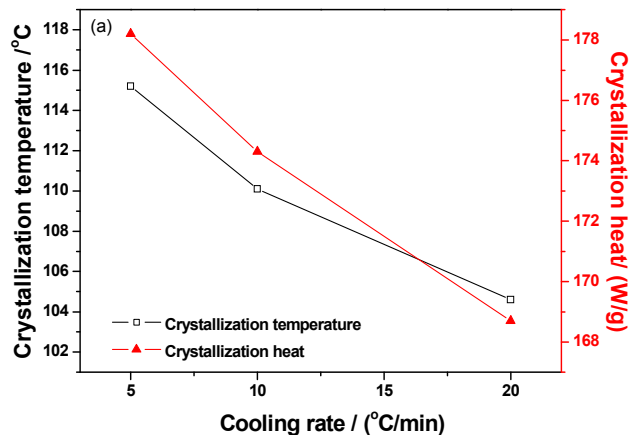
### Characterization

Differential scanning calorimeter (DSC) analyses of the samples are carried out by DSC-2910 (TA Corporation, USA) with a heating rate of  $5^\circ\text{C}/\text{min}$ ,  $10^\circ\text{C}/\text{min}$  and  $20^\circ\text{C}/\text{min}$  under nitrogen atmosphere; Thermal conductive coefficients of the samples are measured using a Hot Disk instrument (AB Corporation, Sweden), which is based upon a transient technique. The measurements are performed with bulk specimens ( $20 \times 20 \times 4 \text{ mm}^3$ ) by putting the sensor (3mm diameter) between two similar slabs of material. The sensor supplies a heat pulse of  $0.03\text{W}$  for 20 seconds to the sample and the associated change in temperature is recorded. And the thermal conductivity of the individual samples is obtained<sup>23</sup>; Scanning electron microscope (SEM) morphologies of the samples are analyzed by VEGA3-LMH (TESCAN Corporation, Czech Republic); Thermo-gravimetric analyses (TGA) of the samples are performed using STA 449F3 thermoanalyzer (Netzsch Group, Germany) in the temperature range of  $40\text{--}650^\circ\text{C}$  with a heating rate of  $10^\circ\text{C}/\text{min}$  under argon atmosphere.

## Results and discussion

### Cooling rate influencing on the crystallization and thermal conductivity

The cooling rate influencing on the crystallization and thermal conductivity of UHMWPE matrix is presented in Fig.2.



Cite this: DOI: 10.1039/c0xx00000x

www.rsc.org/xxxxxx

## ARTICLE TYPE

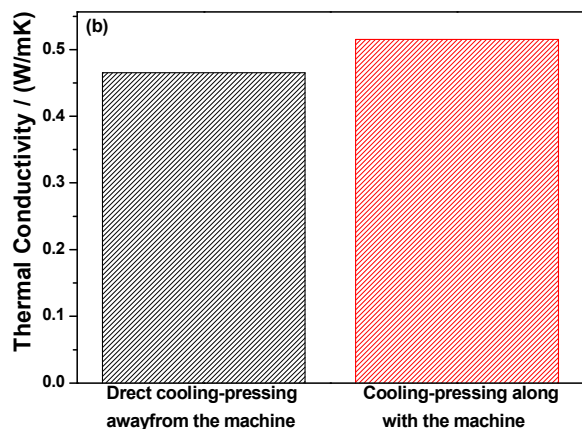


**Fig.2** The cooling rate influencing on the crystallization and thermal conductivity of the UHMWPE matrix. (a) Crystallization; (b) Thermal conductivity

5 With the decrease of cooling rate, the crystallization temperature, crystallization heat and thermal conductivity are all increased. It reveals that the slower cooling rate is, the higher crystallization temperature and crystallization heat are. The reason can be ascribed that, with a slower cooling rate, the crystallization of  
 10 UHMWPE matrix will be more perfect, finally to improve the crystallinity of UHMWPE accordingly, which is beneficial for phonon transmission, resulting in the higher thermal conductivity of UHMWPE matrix.

#### 15 Thermal conductivities of the GNPs/UHMWPE nanocomposites

The volume fraction of GNPs influencing on the thermal conductivities of the GNPs/UHMWPE nanocomposites is shown in Fig.3.

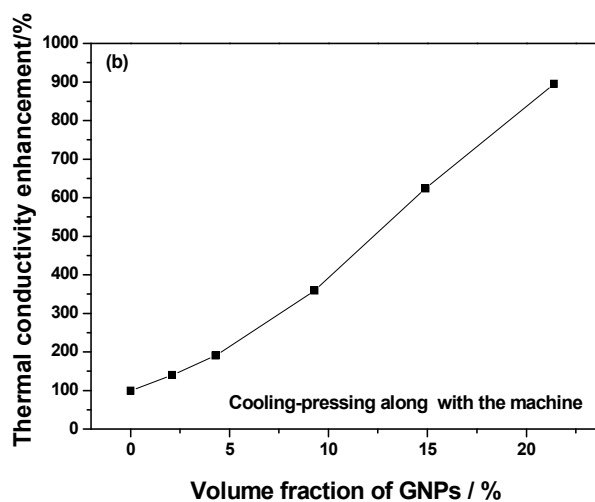
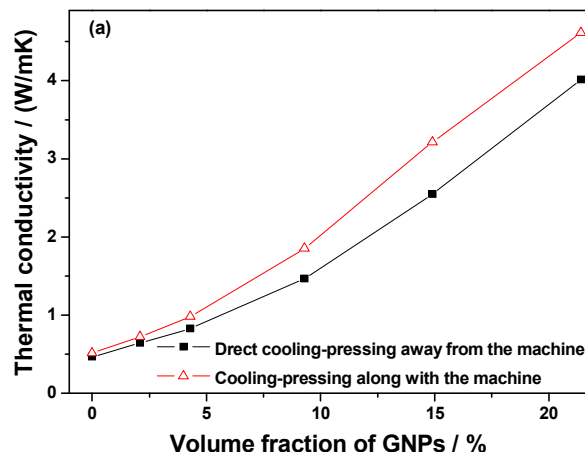
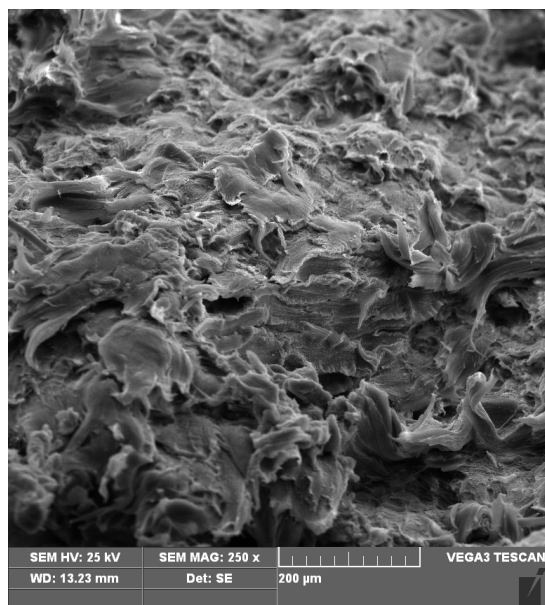


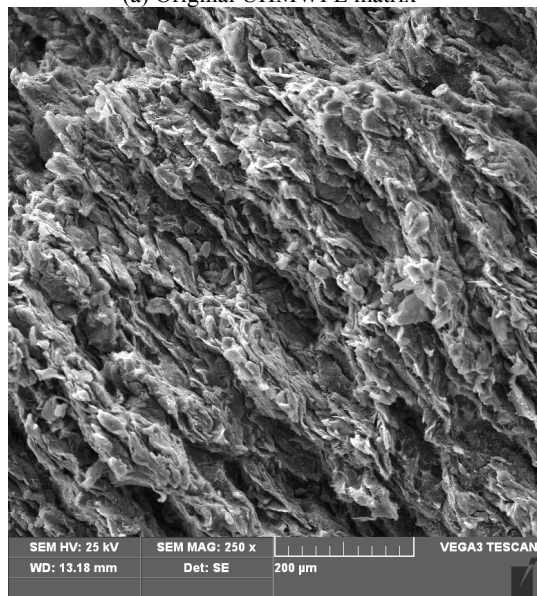
**Fig.3** The volume fraction of GNPs influencing on the thermal conductivities of the GNPs/UHMWPE nanocomposites (a) Thermal conductivity; (b) Thermal conductivity enhancement  
 20 GNPs/UHMWPE nanocomposites exhibit a rapid improvement of the thermal conductivities beyond 4.3 vol% GNPs. And the thermal conductive coefficient of the GNPs/UHMWPE  
 25 nanocomposite with 21.4 vol% (40 wt%) GNPs is greatly improved to 4.624 W/ mK, 9 times higher than that of the original UHMWPE matrix.

30 The high intrinsic thermal conductivity of GNPs can offer reasonable explanations for the higher improvement of thermal conductivities of the GNPs/UHMWPE nanocomposites than that of traditional thermal conductive fillers, and the super diameter/thickness ratio of GNPs can also result in the higher  
 35 improvement of thermal conductivities.

Meanwhile, the thermal conductivities of the GNPs/UHMWPE nanocomposites are strongly depended on the volume fraction of the GNPs in the UHMWPE matrix. GNPs with low volume fraction have weak interaction with each other to present a relatively little increasing thermal conductivities. With the increasing volume fraction of GNPs, the interconnected function of GNPs-GNPs is improved obviously, and the probability of the formation of thermal conductive networks is increased, thus the thermal conductivities of the GNPs/UHMWPE nanocomposites are improved obviously. Moreover, our proposed method can fabricate the GNPs/UHMWPE nanocomposites with segregated structures, easy to form the thermal conductive networks (Fig.1). Fig.4 reveals that the multidimensional thermal conductive networks of GNPs-GNPs are formed with the addition of 21.4 vol% (40 wt%) GNPs.



(a) Original UHMWPE matrix



(b) Nanocomposites with 21.4vol% (40 wt%) GNPs

Fig.4 SEM morphologies of the original UHMWPE matrix and GNPs/UHMWPE nanocomposite with 21.4vol% (40 wt%) GNPs

As also seen form Fig.3, for the same addition of GNPs, the GNPs/UHMWPE nanocomposites via cooling-pressing along with the machine possess relatively higher thermal conductivities.

It is attributed that UHMWPE can crystallize more slowly at a lower cooling rate. Therefore, the corresponding crystallinity and crystal perfection of the UHMWPE matrix are both improved, which are beneficial for phonon transmission, resulting in the higher thermal conductivities.

### Agari's semi-empirical model fitting of the GNPs/UHMWPE nanocomposites

Agari's semi-empirical model can yield better results than the theoretical ones. The logarithmic equation of Agari is shown as follows<sup>47, 48</sup>:

$$\lg \lambda_c = V_f * C_f * \lg \lambda_f + (1 - V_f) \lg(C_p \lambda_p)$$

Where  $C_p$  represents the effect of GNPs on the UHMWPE structure, i.e.  $C_p$  is related to the change of thermal conductivity of UHMWPE matrix, as a consequence of a change of its crystallinity;  $C_f$  represents the ability of GNPs to continuous thermal conductive chains & networks,  $0 < C_f < 1$ .

Fig.5 shows the logarithmic values of thermal conductivities as a function of the GNPs volume fraction.

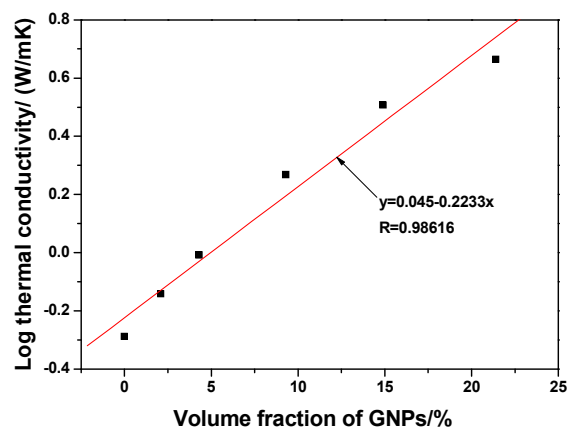


Fig.5 Logarithmic thermal conductivities of the GNPs/UHMWPE nanocomposites as a function of the GNPs volume fraction

The parameters of  $C_p$  and  $C_f$  are calculated to be 1.2851 and 0.761, respectively. The high value of  $C_p$  suggests that the GNPs can influence the crystallinity of the UHMWPE matrix. The low value of  $C_f$  suggests that the GNPs have strong ability to form continuous thermal conductive networks, that is, the formation of thermal conductive networks becomes much easier with the incorporation of GNPs.

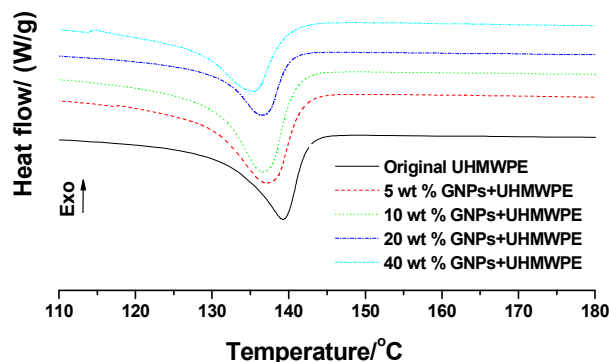
### Thermal properties of the GNPs/UHMWPE nanocomposites

Fig.6 shows the volume fraction of GNPs influencing on the melting heat and melting temperature of the GNPs/UHMWPE nanocomposites by DSC analysis. And the corresponding thermal data are listed in the Table 1.

Cite this: DOI: 10.1039/c0xx00000x

www.rsc.org/xxxxxx

## ARTICLE TYPE



**Fig.6** DSC curves of original UHMWPE and GNP/UHMWPE nanocomposites

**Table 1** Thermal data of original UHMWPE and GNP/UHMWPE nanocomposites from DSC analysis

Samples	Melting heat (J/g)	Melting temperature /°C
Original UHMWPE	158.6	139.1
5 wt% GNP+UHMWPE	156.4	137.2
10 wt% GNP+UHMWPE	147.1	136.8
20 wt% GNP+UHMWPE	149.7	136.5
40 wt% GNP+UHMWPE	145.9	135.4

Both the melting heat and melting temperature of the GNP/UHMWPE nanocomposites are decreased slightly with the increasing addition of GNPs. The corresponding melting heat is decreased from 158.6 J/g (original UHMWPE) to 156.4 J/g (5 wt% GNPs), 147.1 J/g (10 wt% GNPs), 149.7 J/g (20 wt% GNPs) and 145.9 J/g (40 wt% GNPs). Meanwhile, the corresponding melting temperature is also decreased from 139.1°C (original UHMWPE) to 137.2°C (5 wt% GNPs), 136.8°C (10 wt% GNPs), 136.5°C (20 wt% GNPs) and 135.4°C (40 wt% GNPs). It can be attributed that the heterogeneous nucleation of GNPs can hinder the homogeneous nucleation of UHMWPE matrix. Meanwhile, the addition of GNPs can also increase the thickness of crystal plate of UHMWPE system. Common function in above both side, would effectively decrease the heat enthalpy of the GNP/UHMWPE nanocomposites, finally to decrease the crystallinity accordingly.

TGA curves of original UHMWPE matrix and GNP/UHMWPE nanocomposites are presented in **Fig. 7**. And the corresponding characteristic thermal data of original UHMWPE matrix and GNP/UHMWPE nanocomposites are listed in the **Table 2**.

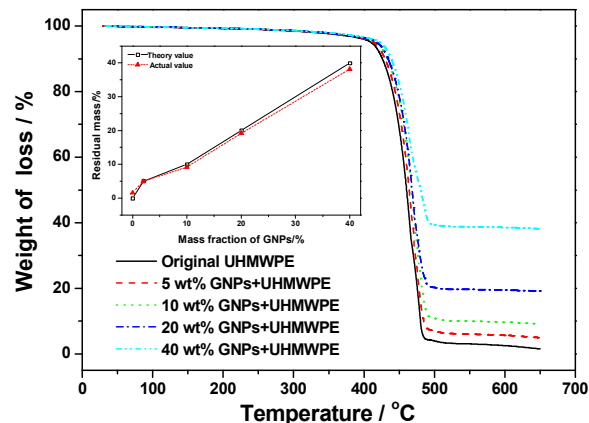


**Fig.7** TGA curves of original UHMWPE and GNP/UHMWPE nanocomposites

**Table 2** Thermal data of original UHMWPE matrix and GNP/UHMWPE nanocomposites from TGA analysis

Samples	Temperature/°C		Heat-resistance index*/°C	Residual mass/%	
	T <sub>5</sub>	T <sub>30</sub>		Theory	Actual
Original UHMWPE	410.3	449.2	212.5	0	1.49
5wt% GNP/ UHMWPE	414.0	452.9	214.3	5	4.98
10wt% GNP/ UHMWPE	417.2	456.1	215.9	10	9.17
20wt% GNP/ UHMWPE	418.3	457.2	216.4	20	19.15
40wt% GNP/ UHMWPE	422.7	461.2	218.4	40	38.15

The corresponding weight loss temperatures are increased at the same stages with the increasing addition of GNPs. And the corresponding heat-resistance index of original UHMWPE and GNP/UHMWPE nanocomposites is 212.5°C, 214.3°C (5 wt% GNPs), 215.9°C (10 wt% GNPs), 216.4°C (20 wt% GNPs) and 218.4°C (40 wt% GNPs), respectively. It suggests that the thermal stabilities of the GNP/UHMWPE nanocomposites are increased. The reason is that GNPs possess higher heat capacity and thermal conductivity compared to original UHMWPE. Therefore, GNPs can preferably absorb the heat, resulting in UHMWPE degraded at higher temperatures. In addition, the actual residual mass value is very close to theory residual mass value, which proves that GNPs are located uniformly on the interface of UHMWPE matrix.

## Conclusion

GNPs are located on the interface of UHMWPE matrix via our proposed method of mechanical ball milling followed by hot-pressing. The thermal conductive coefficient of the GNP/UHMWPE nanocomposite with 21.4 vol% (40 wt%) GNPs is greatly improved to 4.624 W/ mK, 9 times higher than that of original UHMWPE matrix. The significantly high improvement of the thermal conductivity is ascribed to the formation of

multidimensional thermal conductive networks of GNPs-GNPs. Agari's semi-empirical model fitting reveals that GNPs have strong ability to form continuous thermal conductive networks. The cooling-pressing along with the machine is beneficial for increasing the thermal conductivities of the GNPs/UHMWPE nanocomposites by further improving the crystallinity of UHMWPE matrix. Furthermore, the thermal stabilities of the GNPs/UHMWPE nanocomposites are increased with the increasing addition of GNPs.

## 10 Acknowledgments

The authors are grateful for the support and funding from the Foundation of Natural Science Foundation of China (No. 51403175 and No. 81400765); Shaanxi National Science Foundation of Shaanxi Province (No. 2014JQ6203); Space Supporting Fund from China Aerospace Science and Industry Corporation (No. 2014-HT-XGD) and the Fundamental Research Funds for the Central Universities (No. 3102015ZY066).

## References

- [1]Min C, Yu DM, Cao JY, Wang GL, Feng LH. Carbon, 2013, 55: 116-125.
- [2]Zhang YC, Dai K, Tang JH, Ji X, Li ZM. Mater Lett, 2010, 64: 1430-1432.
- [3]Kim K, Kim M, Kim J. Compos Sci Technol, 2014, 103: 72-77.
- [4]Shahil KMF, Balandin AA. Nano Lett, 2012, 12: 861-867.
- [5]Gao LM, Chou T-W, Thostenson ET, Godara A, Zhang ZG, Mezzo L. Carbon, 2010, 48: 2649-2651.
- [6]Luo T, Lloyd JR. Adv Funct Mater, 2012, 22: 2495-2502.
- [7]Liang Q, Yao X, Wang W, Liu Y, Wong CP. ACS Nano, 2011, 5: 2392-2401.
- [8]Losego MD, Grady ME, Sottos NR, Cahill DG, Braun PV. Nat Mater, 2012, 11: 502-506.
- [9]Song SH, Park KH, Kim BH, Choi YW, Jun GH, Lee DJ. Adv Mater, 2013, 25: 732-737.
- [10]Im H, Kim J. Carbon, 2012, 50: 5429-5440.
- [11]Fu YX, He ZX, Mo DC, Lu SS. Int J Therm Sci, 2014, 86: 276-283.
- [12]Heo C, Chang J-H. Solid State Sci, 2014, 24: 6-14.
- [13]Datsyuk V, Trotsenko S, Reich S. Carbon, 2013, 52: 605-608.
- [14]Liu CH, Fan SS. Appl Phys Lett, 2005, 86: 123106-9.
- [15]Kwon SY, Kwon IIM, Kim Y-G, Lee S, Seo Y-S. Carbon, 2013, 55: 285-290.
- [16]Pak SY, Kim HM, Kim SY, Youn JR. Carbon, 2011, 50: 4830-4838.
- [17]Huang XY, Zhi CY, Jiang PK, Golberg D, Bando Y, Tanaka T. Adv Funct Mater, 2013, 23: 1824-1831.
- [18]Zhu Y, Chen KX, Kang FY. Solid State Commun, 2013, 158: 46-50.
- [19]He H, Fu RL, Shen Y, Han YC, Song XF. Compos Sci Technol, 2007, 67: 2493-2499.
- [20]Zhou WY, Wang CF, Ai T, Wu K, Zhao FJ, Gu HZ. Compos Part A, 2009, 40: 830-836.
- [21]Zhou TL, Wang X, Liu XH, Xiong DS. Carbon, 2010, 48: 1171-1176.
- [22]Yang K, Gu MY. Compos Part A, 2010, 41: 215-221.
- [23]Tu HM, Ye L. Polym Adv Technol, 2009, 20: 21-27.
- [24]Vitorino N, Abrantes JC, Frade JR. Mater Lett, 2013, 92: 100-103.
- [25]Li Z, Sun WG, Wang G, Wu ZG. Sol Energy Mater Sol Cells, 2014, 128: 447-455.
- [26]Gu JW, Du JJ, Dang J, Geng WC, Hu SH, Zhang QY. RSC Adv, 2014, 4: 22101-22105.
- [27]Gu JW, Xie C, Li HL, Dang J, Zhang QY. Polym Compos, 2014, 35: 1087-1092.
- [28]Gu JW, Zhang QY, Dang J, Yin CJ, Chen SJ. J Appl Polym Sci, 2012, 124: 132-137.
- [29]Gu JW, Zhang QY, Dang J, Xie C. Polym Adv Technol, 2012, 23: 1025-1028.
- [30]Gu JW, Zhang QY, Dang J, Zhang JP, Yang ZY. Polym Eng Sci, 2009, 49: 1030-1034.
- [31]Gu JW, Zhang QY, Dang J, Zhang JP, Chen SJ. Polym Bull, 2009, 62: 689-697.
- [32]Han Z, Fina A. Prog Polym Sci, 2011, 36: 914-944.
- [33]Yang XD, Wu SH, Song YH. Adhesion, 2012, 33: 75-79.
- [34]Hu M, Yu D, Wei J. Polym Test, 2007, 26: 333-337.
- [35]Stankovich S, Dikin DA, Dommett GHB, Kohlhaas KM, Zimney EJ, Stach EA, et al., Nature, 2006, 42: 282-286.
- [36]Shenogina N, Shenogin S, Xue L, Keblinski P. Appl Phys Lett, 2005, 87: 133106-133106-3.
- [37]Zhang C, Ma CA, Wang P, Sumita M. Carbon, 2005, 43: 2544-2553.
- [38]Gao JF, Li ZM, Meng QJ, Yang Q. Mater Lett, 2008, 62: 3530-3502.
- [39]Sattari M, Naimi-Jamal MR, Khavandi A. Polym Test, 2014, 38: 26-34.
- [40]Chukov DI, Stepashkin AA, Gorshenkov MV, Tcherdyntsev VV, Kaloshkin SD. Journal Alloys Compd, 2014, 586: S459-S463
- [41]Hong JH, Pan ZJ, Yao M, Zhang XY. Synthc Met, 2014, 193: 117-124.
- [42]Nair RR, Blake P, Grigorenko AN, Novoselov KS, Booth TJ, Stauber T. Science, 2008, 320: 1308.
- [43]Liu Q, Liu ZF, Zhang XY, Yang LY, Zhang N, Pan GL, et al., Adv Funct Mater, 2009, 19: 894-904.
- [44]Kuzmenko AB, van Heumen E, F. Carbone F, van der Marel D. Phys Rev Lett, 2008, 100: 117401.
- [45]Zhang LY, Chen GH. Mater Rev, 2011, 25: 85-88.
- [46]Kalaitzidou K, Fukushima H, Drzal LT. Carbon, 2007, 45: 1446-1452.
- [47]Agari Y, Ueda A, Tanaka M, Nagai S. J Appl Polym Sci, 1999, 40: 929-941.
- [48]Agari Y, Ueda A, Nagai S. J Appl Polym Sci, 1991, 43: 1117-1124.